Cell, Vol. 73, 1323–1337, July 2, 1993, Copyright © 1993 by Cell Press

Drosophila Tissues with Different Metamorphic Responses to Ecdysone Express Different Ecdysone Receptor Isoforms

William S. Talbot,* Elizabeth A. Swyryd, and David S. Hogness
Department of Biochemistry
and Department of Developmental Biology
Stanford University School of Medicine
Stanford, California 94305

Summary

In D. melanogaster a pulse of the steroid hormone ecdysone triggers the larval-to-adult metamorphosis, a complex process in which this hormone induces imaginal tissues to generate adult structures and larval tissues to degenerate. We show that the *EcR* gene encodes three ecdysone receptor isoforms (EcR-A, EcR-B1, and EcR-B2) that have common DNA- and hormone-binding domains but different N-terminal regions. We have used isoform-specific monoclonal antibodies to show that at the onset of metamorphosis different ecdysone target tissues express different isoform combinations in a manner consistent with the proposition that the different metamorphic responses of these tissues require different combinations of the EcR isoforms. We have also determined temporal developmental profiles of the EcR isoforms and their mRNAs in whole animals, showing that different isoforms predominate at different developmental stages that are marked by a pulse of ecdysone.

Introduction

Metamorphosis in Drosophila melanogaster is triggered by a pulse of the steroid hormone 20-OH ecdysone, hereafter referred to as ecdysone (reviewed in Riddiford, 1993). In this complete metamorphosis, there is little or no morphological overlap between the initial and final metamorphic states, i.e., between the late third instar larva and the adult fly. This lack of overlap results from the division of most tissues in the late third instar larva into two classes: the imaginal tissues that are hidden inside the larva and generate adult structures in response to the ecdysone pulse at the end of larval life and the strictly larval tissues that provide most of the functional structures of the larva and that degenerate in response to this pulse.

Members of both tissue classes exhibit a wide variety of metamorphic responses to ecdysone. For example, the imaginal tissues that generate the exterior structures of the fly are of two kinds: the small segmentally repeated histoblast nests that generate the abdominal structures and the much larger imaginal discs that produce head and thoracic structures, as well as the genitalia. Individual histoblast nests consist of about a dozen cells that are set aside during embryogenesis, remain quiescent during larval development, and, after the metamorphic ecdysone pulse, proliferate rapidly and migrate to replace the moribund larval epidermis (Madhavan and Schneiderman, 1977; Roseland and Schneiderman, 1979; Riddiford, 1993). By contrast, the imaginal discs consist of thousands of cells that form folded epithelial sacs of little structural distinction, each connected to the larval epidermis by a narrow tubular stalk. While they, too, derive from similarly small clusters of embryonic founder cells within the prospective larval epidermis, the imaginal disc clusters invaginate during embryogenesis (Bate and Martinez-Arias, 1991), grow by cell division during larval development (Madhavan and Schneiderman, 1977), and respond to the metamorphic ecdysone pulse by evagination through the stalk orifice, unfolding into forms that exhibit strong morphological similarities to the adult structures they generate during pupal development (Fristrom et al., 1977; Condic et al., 1991).

The imaginal tissues that generate certain internal organs of the adult exhibit a similar variety of ecdysone responses. Thus, the imaginal rings that generate the adult foregut, hindgut, and salivary glands in response to ecdysone bear a certain resemblance to the imaginal discs in that they, too, achieve their considerable size by cell division during larval development (Madhavan and Schneiderman, 1977). A closer parallel can be drawn between the histoblast nests and the small clusters or islands of imaginal cells that decorate the outer surface of the larval midgut since these midgut islands respond to ecdysone by rapid cell proliferation and migration to generate the adult midgut (Bodenstein, 1950; Madhavan and Schneiderman, 1977).

These differences in the metamorphic response of imaginal tissues to ecdysone, as well as differences in the degenerative response of larval tissues to this steroid, evoke a fundamental question about metamorphosis: how can a single hormone induce a variety of tissue responses? We address this question here in the context of the genetic regulatory hierarchies that determine these responses. Perception of these hierarchies came first from studies on the effects of ecdysone on the pattern of transcription puffs in the polytene chromosomes of larval salivary glands. These studies culminated in a hierarchical model in which ecdysone binds to its receptor to form an ecdysone–receptor complex that acts oppositely on two sets of genes, inducing the transcription of a half-dozen early genes and repressing the transcription of a much larger set of late genes. The early genes encode transcription factors that also act oppositely on these two gene sets, inducing the late genes and repressing the early genes (Ashburner et al., 1974).

Several postulates of this model have been confirmed by results obtained from the cloning and characterization of three early genes: *E74* (Burtis, 1985; Burtis et al., 1990; Thummel et al., 1990), *E75* (Segraves, 1988; Segraves and Hogness, 1990), and *Broad-Complex* (*BR-C*) (DiBello

*Present address: Institute of Neuroscience, University of Oregon, Eugene, Oregon 97403.

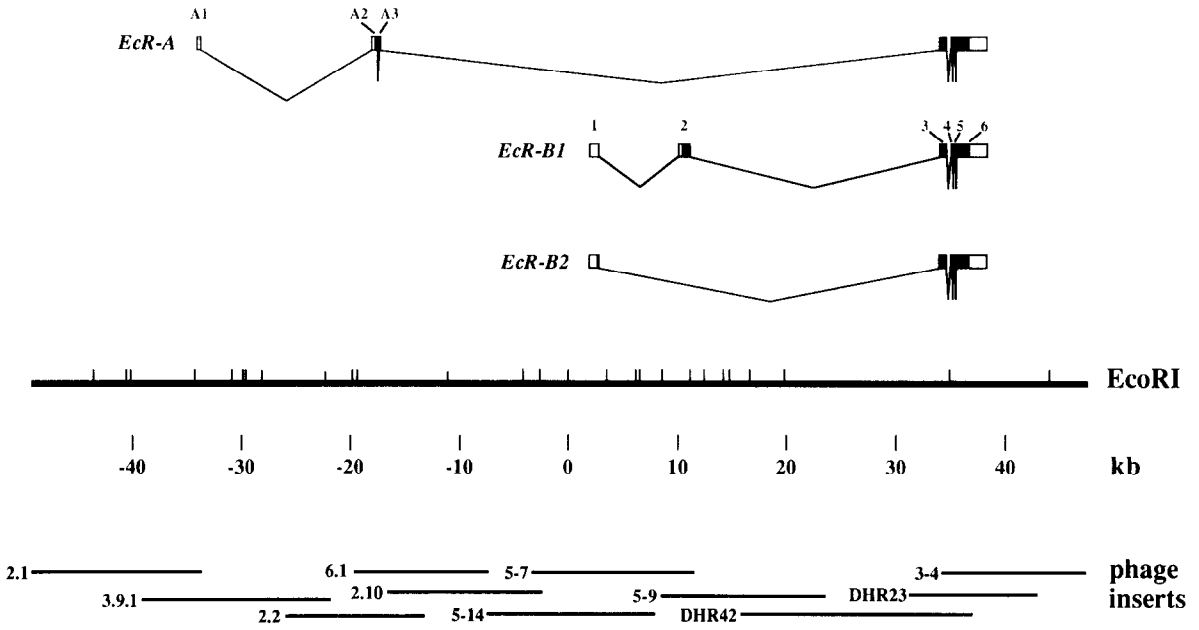

Figure 1. Genomic Structure of *EcR*

The positions of exons mapped by comparison of genomic clones with *EcR-A*, *EcR-B1*, and *EcR-B2* cDNA clones are shown at the top. Coding regions are shaded, and the 5′ ends of the *EcR-A* and *EcR-B* transcription units are to the left. The translational initiation codon of the *EcR-B2* ORF is encoded in exon 1. The *EcR-B1* ORF does not begin at the *EcR-B2* initiation codon because of stop codons in the 5′ portion of exon 2. EcoRI sites in the genomic DNA are indicated by the short vertical marks on the thick line above the kilobase scale. The kilobase coordinates follow the convention of Koelle et al. (1991). Because the 3′ ends of the *EcR* mRNAs have not been mapped, there may be additional noncoding sequences in the 3′ untranslated regions of these transcripts. The structure of the *EcR-B1* mRNA and the portion of the genomic map defined by phages 5–14 through 3–4 were described by Koelle et al. (1991).

et al., 1991). All three encode proteins identifiable by sequence, and in certain cases by function, as DNA-binding members of transcription factor families. Early gene promoters are activated by ecdysone in a primary response. That activation is subsequently repressed in the continued presence of ecdysone. Finally, the postulate that early gene proteins regulate the transcription of late genes is supported by the observations that the E74A protein binds to late gene puff sites (Urness and Thummel, 1990) and that the transcription of a set of cloned late genes is decreased in *BR-C* mutants (Guay and Guild, 1991).

The cloning of the early genes also led to the discovery that they are ecdysone-induced in other tissues, both larval and imaginal. This discovery led to an extension of the Ashburner model called the tissue coordination model (Burtis et al., 1990; Thummel et al., 1990). In this model, the different target tissues respond to ecdysone by the activation of genetic regulatory hierarchies akin to that proposed by Ashburner et al. (1974) for the larval salivary gland. Differences in these tissues in their metamorphic responses were proposed to result in large part from different but overlapping combinations of the transcription factors encoded by the early genes. The question of what determines these differences in early gene proteins was left open, but an obvious possibility is that they result from different combinations of different ecdysone receptor proteins. It is this possibility that we address here.

The Drosophila *EcR* gene has recently been found to encode an ecdysone receptor protein, EcR (Koelle et al., 1991). EcR binds to and is required for the activation of an ecdysone response element, a DNA sequence that can confer ecdysone inducibility on an otherwise nonresponsive promoter. Koelle et al. (1991) also showed that EcR is required for the formation of an ecdysone–receptor complex and that its amino acid sequence further qualifies it as a full-fledged member of the steroid receptor superfamily by virtue of homologies to their conserved DNA- and hormone-binding domains. More recently, it has been shown that EcR binds to DNA as a heterodimer with the USP protein, another member of this superfamily encoded by the Drosophila *ultraspiracle* (*usp*) gene (Koelle, 1992; Yao et al., 1992; Koelle et al., 1993; Thomas et al., 1993). More remarkably, it appears that ecdysone binding is also dependent upon both proteins (Koelle, 1992; Koelle et al., 1993).

In principle, therefore, tissue-specific variation in ecdysone receptor function could result from change in the EcR protein or in its pairing partner. There is as yet no significant evidence for the latter proposition. We show here, however, that EcR proteins come in three different forms. More specifically, we show that the *EcR* gene encodes three functional isoforms (EcR-A, EcR-B1, and EcR-B2) that have common DNA- and hormone-binding domains and are distinguished by different N-terminal regions. We further observe that at the onset of metamorphosis, different target tissues express different isoform

combinations in a manner consistent with the proposition that different EcR isoform combinations are required for different metamorphic responses to ecdysone.

Results

EcR Encodes Multiple Messenger RNAs

Preliminary ribonuclease protection experiments (data not shown) suggested that *EcR* encodes novel messenger RNAs (mRNAs) lacking the second exon of the previously identified *EcR* transcript (Koelle et al., 1991), which is designated *EcR-B1* in Figure 1. To identify cDNAs corresponding to these previously uncharacterized *EcR* mRNAs, we screened a cDNA library made from third instar larval tissues with exon-specific probes to identify clones containing exon 3 sequences and lacking those from exon 2 (Figure 1; exons are designated here and below according to the *EcR-B1* structure). Characterization by restriction endonuclease mapping, hybridization analysis, and partial sequencing indicates that the novel *EcR* cDNAs isolated in this screen are of two types differing at their 5′ termini. We have isolated multiple independent cDNA clones of each type (four for *EcR-A* and two for *EcR-B2*), confirming that both of these cDNA classes represent bona fide *EcR* mRNAs. The cDNAs in the first class, which we designate *EcR-B2*, contain exon 1 spliced to exon 3 and thus represent an mRNA that differs from the *EcR-B1* transcript because of alternative splicing (Figure 1). High resolution restriction endonuclease mapping indicates that *EcR-B1* and *EcR-B2* are colinear from exons 3–6.

The cDNAs in the second class represent another novel *EcR* mRNA, which we name *EcR-A*. The *EcR-A* cDNAs lack sequences encoded by exons 1 and 2 and have instead ~1 kb of new material upstream of exon 3. They are colinear with *EcR-B1* and *EcR-B2* from exons 3–6 (Figure 1). *EcR-A*-specific cDNA fragments were used as hybridization probes to screen a Drosophila genomic DNA library to identify the exons encoding these sequences. The *EcR* chromosomal walk reported by Koelle et al. (1991) was then extended to include these *EcR-A* genomic clones (Figure 1). The sequences of the *EcR-A*-specific portion of an *EcR-A* cDNA clone (pWT57) and the corresponding genomic fragments were determined and compared to deduce the number and positions of the *EcR-A* exons (Figures 1 and 2). The first *EcR-A*-specific exon is located ~35 kb upstream of exon 1 in the *B* transcription unit; the total length of the *EcR* gene is therefore ~73 kb. The three *EcR-A* exons (A1, A2, and A3; see Figure 1) are bordered by the appropriate consensus splice donor and acceptor sequences (Mount, 1982) and are separated by two introns, one of ~15 kb and the other of 74 bp.

The genomic positions of the 5′ termini of the *EcR-A*, *EcR-B1*, and *EcR-B2* cDNAs suggested that these mRNAs are transcribed from two different promoters, with *EcR-A* produced from a promoter upstream of the one that produces the two *EcR-B* mRNAs. By mapping the 5′ ends of these transcripts, we confirmed that the *EcR-A* and *EcR-B* mRNAs indeed arise from two overlapping transcription units with distinct promoters. The results of the *EcR-A* and *EcR-B* primer extension analyses presented in Figure 2C indicate that each of these mRNAs has two start sites at adjacent nucleotides, which are indicated in the sequences shown in Figures 2A and 2B. The transcriptional initiation sites determined by primer extension were confirmed by ribonuclease protection analyses (Talbot, 1993).

The *EcR* mRNAs Encode Distinct EcR Proteins

The *EcR-A*, *EcR-B1*, and *EcR-B2* mRNAs have different 5′ regions (see Figure 1), and they are predicted to encode three different proteins with distinct N-terminal sequences of 197, 226, and 17 residues in length, respectively (Figures 2A and 3A; Koelle et al., 1991). Figure 3A shows a schematic of the three EcR proteins indicating that they share a 652 residue C-terminal common region that contains the DNA- and hormone-binding domains characteristic of members of the steroid receptor superfamily (for detailed sequence comparisons, see Koelle et al., 1991). The isoform-specific N-terminal regions are not significantly similar to each other or to other protein sequences in the data base.

We have produced isoform-specific monoclonal antibodies that recognize the N-terminal segments of the EcR-A and EcR-B1 proteins, as well as common region monoclonal antibodies that detect all three of the EcR isoforms (Table 1; see Experimental Procedures for details of antibody production). The immunoblots presented in Figure 3B demonstrate the specificity of representative anti-EcR monoclonal antibodies. Extracts of Drosophila S2 cells that had been transiently transfected with EcR-A, EcR-B1, or EcR-B2 expression constructs (Figure 3B, lanes 2, 3, and 4, respectively) or, as a control, the expression vector alone (lanes 1) were probed with isoform-specific and common region anti-EcR monoclonal antibodies. The anti-EcR-A antibody detects a 105 kd protein that is present only in the S2 cells transfected with the EcR-A expression construct (Figure 3B, anti-EcR-A). The anti-EcR-B1 antibody also detects a 105 kd protein, indicating that the EcR-A and EcR-B1 proteins comigrate in SDS–polyacrylamide gel electrophoresis (Figure 3B, anti-EcR-B1; the predicted sizes of the EcR-A and EcR-B1 proteins are 91.2 kd and 93.8 kd, respectively). EcR-B1 is present in the control S2 cells (Figure 3B, lane 1), which is consistent with our previous finding that this protein is required for the endogenous ecdysone receptor activity in these cells (Koelle et al., 1991) and is expressed at a higher level in S2 cells transfected with the EcR-B1 expression plasmid (lane 3). EcR-B2 is detected by the common region antibody as an 80 kd protein that is present only in S2 cells that have been transfected with the EcR-B2 expression construct (Figure 3B, anti-common; the predicted size of EcR-B2 is 73.4 kd). The EcR-B2 protein is not recognized by either the EcR-A or EcR-B1 antibody, further confirming the isoform specificity of these antibodies. Additional confirmation of these specificities derives from tissue staining experiments with *EcR* mutants: AD4.4 (anti-B1) staining is greatly reduced in animals bearing stop codon mutations in the *EcR-B1*-specific exon, and 15G1a (anti-A) staining is absent in mutants lacking the *EcR-A*-specific exons (M. Bender, W. S. T., and D. S. H., unpublished data). As might be expected from its short N-terminal iso-

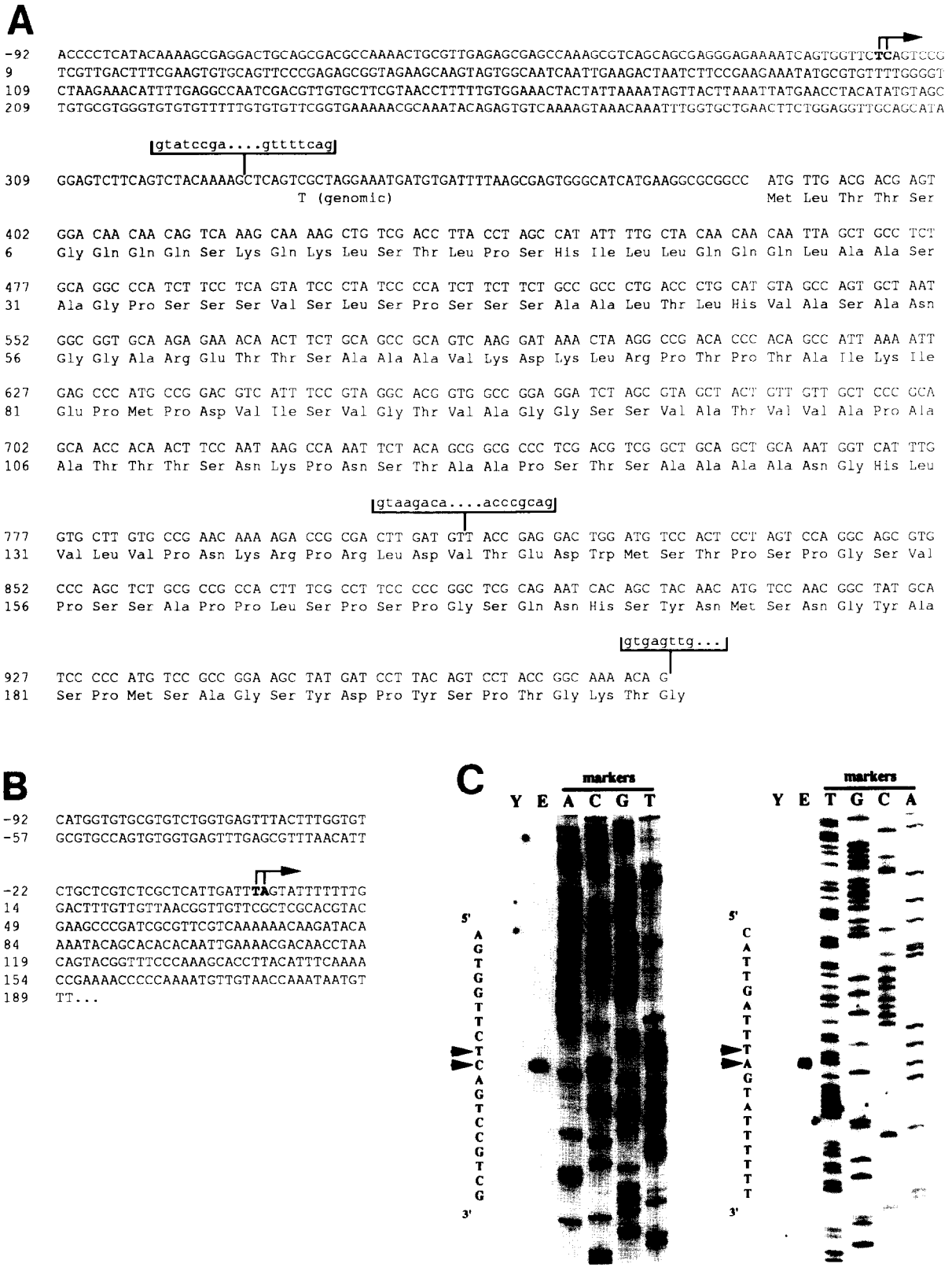

Figure 2. Sequence and 5′ End Analysis of the *EcR-A* and *EcR-B* Transcription Units

(A) Composite cDNA and genomic DNA sequence of the *EcR-A*-specific region. Numbers at the left refer to nucleotide and predicted amino acid sequence; nucleotide sequence coordinates begin with +1 as the first of the two transcription start sites identified in (C). The positions of introns are indicated above the sequence, with the splice donor and acceptor sequences shown in lowercase type. Nucleotides +17 through +978 derive from the pWT57 *EcR-A* cDNA clone; other sequences were obtained from genomic clones. A mismatch between the cDNA and genomic sequences

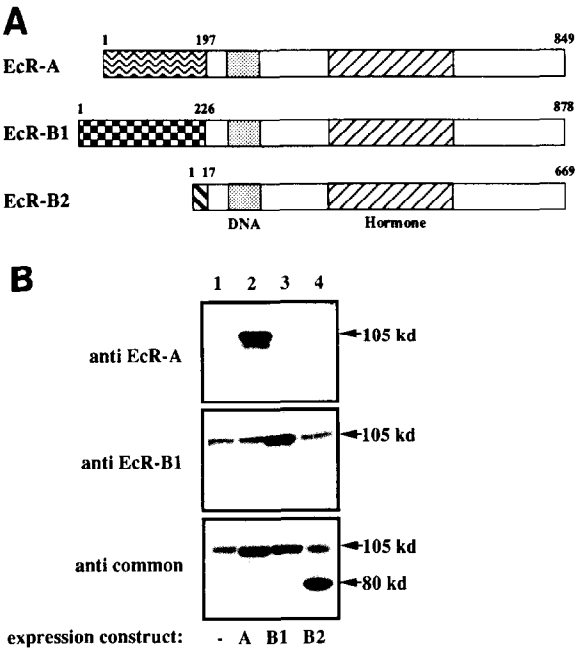

Figure 3. Anti-EcR Monoclonal Antibodies Detect EcR Proteins Expressed in Drosophila S2 Cells

(A) Schematic representations of the EcR isoforms. The EcR common region contains the DNA- and hormone-binding domains, as defined both by the homology of these regions to other members of the steroid receptor superfamily and by functional characterization of EcR chimeras (Christopherson et al., 1992). The common region extends from Gly-227 to Ala-878 of EcR-B1 (Koelle et al., 1991). The predicted sequence of the EcR-A-specific region is given in Figure 2A. The predicted sequence of the EcR-B2-specific region is MDTCGLVAELAHYIDAY.

(B) Detection of EcR proteins in Drosophila S2 cells transfected with EcR expression vectors. S2 cells were transiently transfected with the EcR expression plasmids pAct/EcR-A/2 (lanes 2), pAct/EcR-B1 (lanes 3), or pAct/EcR-B2 (lanes 4); control cells were transfected with the pAct/SV40/BS expression vector lacking EcR sequences (lanes 1). Immunoblots bearing extracts from these transfected cells were probed with the EcR-A-specific monoclonal antibody 15G1a (top panel), the EcR-B1-specific monoclonal antibody AD4.4 (middle panel), or the common region monoclonal antibody DDA2.7 (bottom panel). These antibodies are defined in Table 1. EcR-B1 is present in the control cells, consistent with the finding that EcR-B1 is required for the endogenous ecdysone receptor activity of S2 cells (Koelle et al., 1991). The apparent molecular sizes of the EcR proteins were determined by comparison to the following protein standards: myosin (200 kd), β-gal (116 kd), phosphorylase b (97 kd), and bovine serum albumin (66 kd). The minor band detected with the anti-EcR-A and anti-common antibodies in EcR-A-overproducing extracts is thought to be an EcR-A breakdown product.

form-specific region, anti-EcR-B2 antibodies have not yet been obtained.

The EcR Isoforms Are Functional Ecdysone Receptors

We have previously demonstrated that ecdysone-resistant Drosophila S2 cells contain greatly reduced levels of high affinity ecdysone binding activity relative to normal, ecdysone-sensitive S2 cells (Koelle et al., 1991). Such ecdysone-resistant cells can support only a low level of ecdysone induction of an ecdysone-responsive reporter construct that is highly induced in ecdysone-sensitive cells. This reduction in ecdysone responsiveness is correlated with a diminished expression of the EcR-B1 protein that is normally present in S2 cells, and overexpression of the EcR-B1 protein in these ecdysone-resistant cells restores their ability to support the high level ecdysone induction of the ecdysone-responsive reporter construct (Koelle et al., 1991). Table 2 demonstrates that expression of either EcR-A or EcR-B2 also confers ecdysone responsiveness on the ecdysone-resistant S2 cell line, indicating that these two EcR proteins also function as ecdysone receptors.

The EcR-A and EcR-B1 Isoforms Exhibit Different Tissue Expression Patterns at the Onset of Metamorphosis

To explore the possibility that different combinations of the EcR isoforms are required for the different developmental responses to ecdysone among the target tissues, we have determined the tissue distributions of EcR-A and EcR-B1 at the onset of metamorphosis. For the majority of these immunolocalization experiments (Figures 4–6), tissues were stained with isoform-specific antibodies (anti-A and anti-B1) after dissection from white prepupae, the stage when the metamorphic ecdysone pulse has reached a maximum. While EcR-A and EcR-B1 can both be detected in the nuclei of most tissues at this stage, tissues that stain strongly with antibody against one EcR isoform generally stain weakly with antibody against the other. Apparently, the A and B1 isoforms are expressed in approximately complementary patterns at the onset of metamorphosis.

With one notable exception, the strictly larval tissues exhibit strong anti-B1 staining and weak anti-A staining. Figures 4–6 show that this is the case for the larval fat body (Figures 4C and 4D), muscle (Figures 4E and 4F), foregut (Figures 5A and 5B), midgut (Figures 5A–5D, 6A,

identified at position +336 is indicated. The *EcR-A*-specific nucleotide sequence presented here splices to the common region, which begins at nucleotide 1748 of the *EcR-B1* cDNA sequence (Koelle et al., 1991). Thr-197 is the last EcR-A-specific amino acid residue; the EcR protein common region begins at Gly-198 according to the EcR-A coordinates given here and at Gly-227 of the EcR-B1 protein sequence (Koelle et al., 1991).

(B) Genomic sequence of the 5′ region of the *EcR-B* transcription unit. Numbers at the left refer to the nucleotide sequence of a genomic clone that spans the *EcR-B* transcription start site (position +1) defined in (C). The *EcR-B1* cDNA sequence reported previously begins at nucleotide +82 of the genomic sequence shown here (Koelle et al., 1991).

(C) Primer extension analysis of the *EcR-A* and *EcR-B* transcription units. After annealing to poly(A)$^+$ RNA isolated from Drosophila embryos (lanes E) or yeast total RNA (lanes Y), oligonucleotides complementary to *EcR-A* (left panel) and *EcR-B* (right panel) were used as templates for reverse transcription (see Experimental Procedures). The same primers were used on the appropriate genomic clones to generate the dideoxy sequencing ladders shown in the marker lanes. The marker lanes are designated with respect to the coding strands of the *EcR-A* and *EcR-B* transcripts. The 5′ ends of *EcR-A* and *EcR-B* are indicated in the sequences adjacent to the autoradiograms and also in (A) and (B) above. Because of a band compression, the C residue at +6 of the *EcR-A* sequence is not readily apparent on this autoradiogram (left panel), but it can be clearly visualized on gels run under more highly denaturing conditions and on the other strand.

Table 1. Specificity of Anti-EcR Monoclonal Antibodies

Specificity	Antibody	Location of Epitope[a]
EcR-A	15G1a	15–152
	18F6	15–152
	12H4	15–152
EcR-B1	AD4.4	68–222
Common	GGD11.6	227–331
	EEC11.1	227–331
	AG9.2	227–331
	JG6.2	227–331
	DDA2.7	335–393
	IID9.6	335–393
	AAA5.4	335–393
	AC12.4	649–878
	AG10.2	649–878

[a] For EcR-A-specific antibodies, the epitope locations refer to the amino acid sequence presented in Figure 2A. For EcR-B1-specific and common region antibodies, the locations refer to the sequence of the EcR-B1 protein reported by Koelle et al. (1991).

and 6B), salivary gland (Figures 5E and 5F), and epidermis (Figures 6C–6F). The exception is the prothoracic gland, which exhibits a reciprocal pattern with particularly strong anti-A staining (Figures 4G and 4H). It is curious, and perhaps significant, that this exception is the site of ecdysone biosynthesis during the larval and early pupal stages of development (Sakurai and Gilbert, 1990; Riddiford, 1993). In the lepidopteran Manduca sexta, ecdysone acts directly on the prothoracic gland to inhibit its own biosynthesis (Sakurai and Williams, 1989), raising the possibility that this exceptional EcR isoform expression pattern is required for this feedback regulation.

The staining patterns for the imaginal tissues are interesting because they divide into two classes that correspond to the two classes noted in the Introduction: the large imaginal discs and rings that achieve their size by cell division during larval development (Madhavan and Schneiderman, 1977) and the small cell clusters represented by the histoblast nests and midgut imaginal islands that respond to ecdysone by extensive cell multiplication and migration to generate the adult midgut and abdominal epidermis, respectively (Bodenstein, 1950; Madhavan and Schneiderman, 1977; Roseland and Schneiderman, 1979). Thus, the first of these classes exhibits strong anti-A staining and weak anti-B1 staining, the reciprocal of that observed for the larval tissues. Figures 4A and 4B show that this is the case for the wing imaginal disc, and similar results were obtained with other discs (data not shown; see the legend to Figure 4). This rule also holds for the imaginal rings that generate the foregut (Figures 5A and 5B), hindgut (Figures 5C and 5D), and salivary gland (Figures 5E and 5F) of the adult. By contrast, the second class exhibits moderate to high anti-B1 staining and no detectable anti-A staining, as shown both for the midgut islands (Figures 6A and 6B) and for the histoblast nests (Figures 6C–6F). Although similar to the larval staining pattern, this pattern may be unique if indeed these tissues do not express any of the EcR-A isoform (see the legend to Figure 6).

Temporal Developmental Profiles of *EcR* Expression

In the last section of these Results, we examine the expression of the *EcR-A* and *EcR-B1* mRNAs and proteins in whole animals throughout development (Figure 7). This examination was motivated by previous observations that certain early gene mRNAs, notably *E74A* (Thummel et al., 1990) and *E75A* (Segraves, 1988), are expressed not only at the end of the third larval instar, but also at the five other stages characterized by an ecdysone pulse, namely, at midembryogenesis, in the latter part of the first and second larval instars, and during the pupal and prepupal stages (Richards, 1981). These observations induced Burtis et al. (1990) to postulate that the tissue coordination model also applied to the ecdysone responses of target tissues at these stages. If so, one would expect that one or another of the EcR isoforms would be expressed at these stages and that, for a given stage, one isoform might predominate over another. For example, at the end of the third larval instar, when the metamorphic ecdysone pulse peaks, we can predict from the tissue distributions of the EcR-A and EcR-B1 isoforms presented in the preceding section that EcR-B1 should predominate over EcR-A in whole animals, and presumably the same would be true of their mRNAs. This prediction follows from the observation that the polyploid or polytene nuclei of larval tissues generally stain much more strongly with anti-B1 than anti-A antibodies and from the predominance of larval nuclei over the diploid imaginal nuclei (where EcR-A staining can be the stronger), particularly in genome equivalents of DNA.

The 108–120 hr sample of the developmental Northern analysis given in Figure 7A and the equivalent L3-4 sample of the developmental Western analysis given in Figure 7B conform to this prediction. Thus, the strongest of the 6 kb *EcR-B1* mRNA peaks occurs in this sample at the end of the third larval instar, while the 5 kb *EcR-A* mRNA exhibits a weak peak at this time. (This mRNA presumably corresponds to the *EcR-A* cDNA sequence presented in Figure 2, since it is the only *EcR-A* mRNA detected in late larvae, the stage from which the cDNA library was prepared.) Similarly, the 105 kd EcR-B1 protein and its degradation products are easily detected at this time, while the 105 kd

Table 2. The EcR Proteins Confer Ecdysone Responsiveness on Ecdysone-Resistant Cells

Expression Plasmid	Fold Ecdysone Induction
pUC18	9 ± 1
EcR-A	131 ± 43
EcR-B1	148 ± 50
EcR-B2	168 ± 2

Ecdysone-resistant S2 cells were cotransfected with the ecdysone response reporter plasmid pEcRE/Adh/βgal and either an EcR expression plasmid or, as a control, pUC18. Each transfected culture was split into two dishes, one of which was treated with ecdysone while the other was not. Cell extracts were prepared and assayed for β-gal activity. The specific activities of ecdysone-treated and untreated samples were compared to determine fold ecdysone induction. The mean and range of the fold ecdysone induction values from duplicate transfections are given.

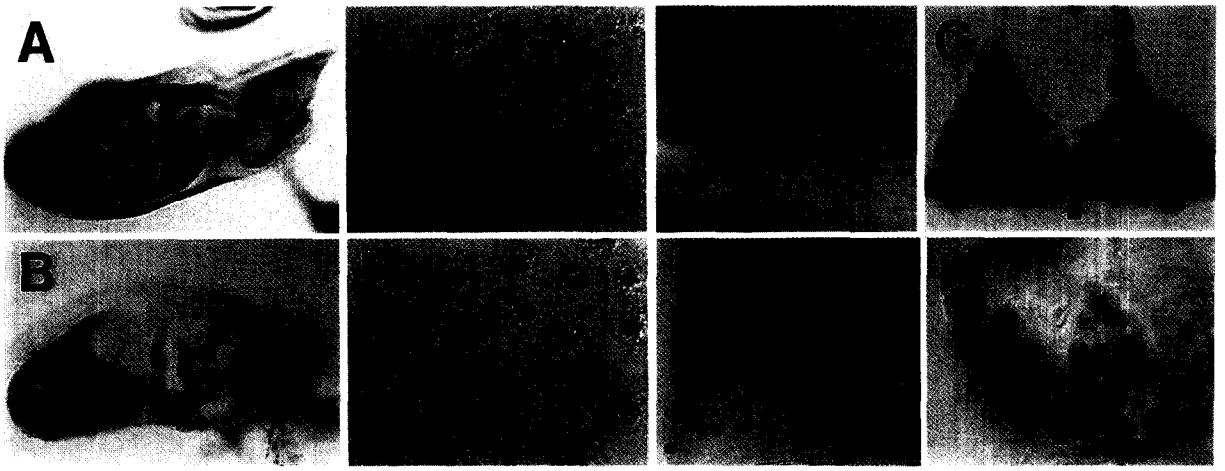

Figure 4. Expression of EcR-A and EcR-B1 in Imaginal Discs and Various Larval Tissues at the Onset of Metamorphosis

Immunolocalization of EcR-A (top row) and EcR-B1 (bottom row) in the wing imaginal disc (A and B), fat body (C and D), muscle (E and F), and ring gland (G and H). EcR-A is expressed at high levels in the wing imaginal disc (A) and in other imaginal discs, including the leg discs, the haltere disc, the labial disc, and the eye–antennal disc (data not shown). Lower levels of EcR-A are detected in the fat body (C) and muscle (E). With the exception of the peripodial membrane, EcR-B1 is expressed at a low level in the wing imaginal disc (B) and in the other imaginal discs noted above (data not shown). Fat body (D) and muscle (F) are heavily stained by the anti-EcR-B1 monoclonal antibody. The cells of the prothoracic gland (large laterally positioned cells in [G]), one of the three tissues comprising the compound ring gland, express very high levels of EcR-A; the corpus allatum (the medial cluster of small cells marked with an arrow in [G]) expresses EcR-A at a lower level. Both of these ring gland tissue types express less EcR-B1 (H) than the fat body (D) and muscle (F). The third tissue in the ring gland, the corpus cardiacum, expresses a very low level of both EcR-A and EcR-B1 (data not shown). All tissues were dissected from white prepupae. We have noted that larval tracheae and the Malpighian tubules express relatively high levels of EcR-B1 and low levels of EcR-A (data not shown). To eliminate variability in staining conditions, the tissues treated with the EcR-A-specific monoclonal antibody 15G1a (A, C, E, and G) were stained together in the same immunohistochemical reaction. Similarly, the tissues treated with the EcR-B1-specific antibody AD4.4 (B, D, F, and H) were stained together.

EcR-A protein is not (Figure 7B; a low level of EcR-A was observed at this time on longer exposure).

A similarly strong but reciprocal difference in the expression of the EcR-A and EcR-B1 proteins was observed during the first 3 hr of embryogenesis (Figure 7B, sample E-1), when there is no ecdysone pulse. This difference is also registered by the respective mRNAs (Figure 7A, 0–3 hr), except that the primary mRNA registered by the *EcR-A*-specific probe is 4 kb rather than 5 kb long. The structure of this mRNA has not been fully characterized, but preliminary ribonuclease protection experiments (Talbot, 1993) indicate that it contains the coding sequence for the 105 kd EcR-A protein and thus represents a second *EcR-A* mRNA. The observation that a 105 kd protein is the only polypeptide prominently recognized by an anti-EcR-A antibody in 0–3 hr embryos supports this possibility (Figure 7B). The ribonuclease protection experiments further indicate that this 4 kb mRNA lacks the first of the *EcR-A*-specific exons (see Figure 1). This result and the early embryonic expression of this transcript suggest that it may be a maternal mRNA transcribed from another promoter active during oogenesis.

This 4 kb *EcR-A* mRNA decreases rapidly, to be replaced by the 5 kb *EcR-A* mRNA that peaks at midembryogenesis (Figure 7A, 12–15 hr) in approximate coincidence with the first ecdysone pulse. The almost constant abundance of the 105 kd EcR-A protein during the first 15 hr of embryogenesis (Figure 7B, samples E1–E5) can be ascribed to the translation of these two mRNA populations. Indeed, a possible function of the putative maternal 4 kb *EcR-A* mRNA is to provide an ecdysone receptor that, when complexed with the ecdysone produced at midembryogenesis, activates the zygotic *EcR-A* and *EcR-B* promoters (see Figures 1 and 2) to produce the midembryonic peaks of the 5 kb *EcR-A* and 6 kb *EcR-B1* mRNAs. This possibility is consistent with the results of Karim and Thummel (1992) that suggest that *EcR* transcription is inducible by ecdysone.

The *EcR-A* and *EcR-B1* mRNAs peak at 18–21 hr of embryogenesis (Figure 7A), and the corresponding increases in the respective proteins at the end of embryogenesis (Figure 7B) are curious because they overlap peaks of *E74A* and *E75A* early gene expression, even though no increase in ecdysone titer has been detected at this time (Richards, 1981). We have commented previously on the possibility that these late embryonic peaks of *EcR* and early gene expression may be indicative of the action of ecdysteroids other than 20-OH ecdysone (Koelle et al., 1991).

This late embryonic expression of the EcR-A protein may account for its presence during the first larval instar (Figure 7B, samples L1-1 and L2) since little or no *EcR-A* mRNA was detected during either the first or second larval instars (Figure 7A, 24–72 hr). By contrast, there appear to be two weak peaks of *EcR-B1* mRNA near the ends of the first and second larval instars (Figure 7A, 36–48 hr and 60–72 hr) that correspond to two small ecdysone pulses. The first of these mRNA peaks might account for the apparent increase in the EcR-B1 protein at the end of the first instar (Figure 7B, sample L1-2). A weak peak of

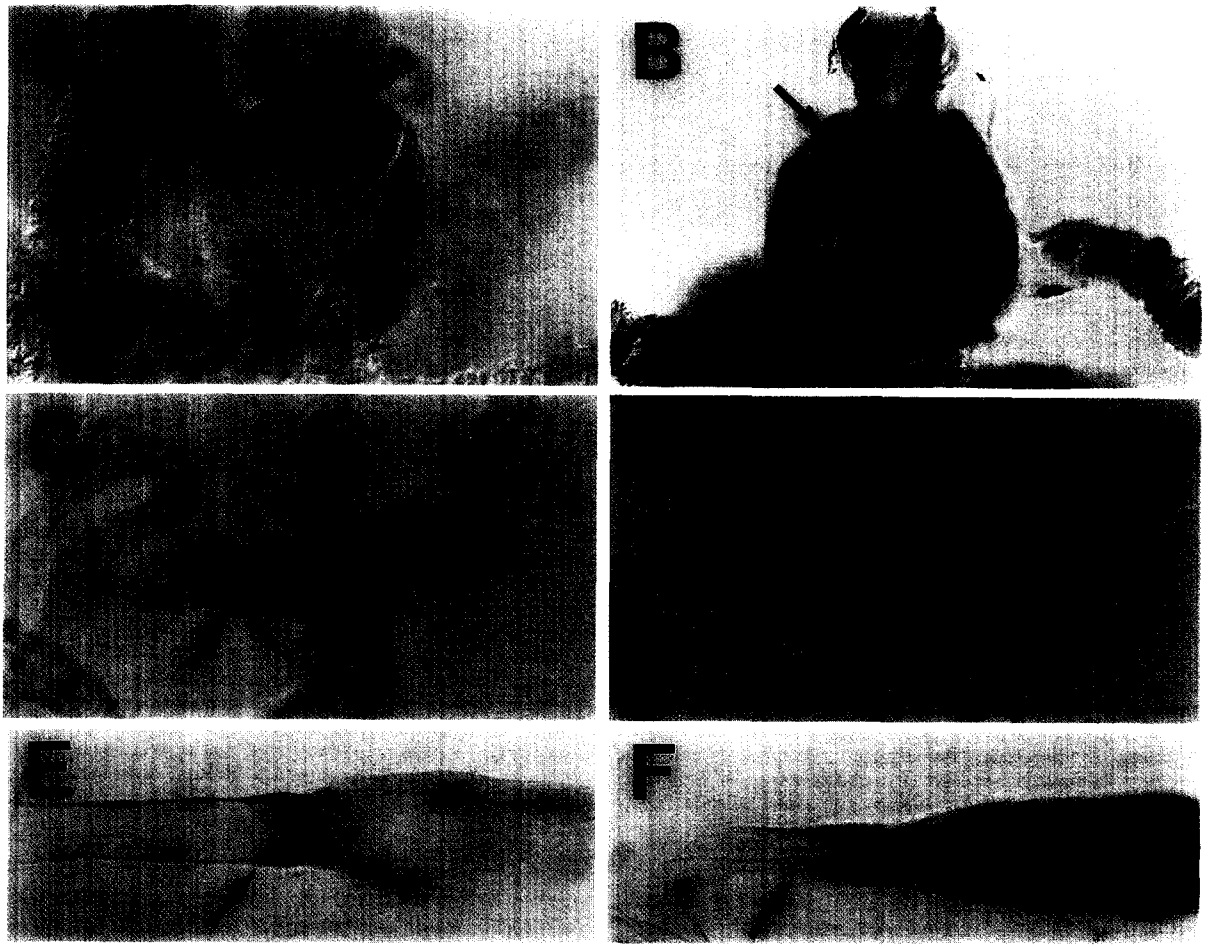

Figure 5. EcR-A and EcR-B1 Expression in the Imaginal Rings and Associated Larval Tissues

Immunolocalization of EcR-A (A, C, and E) and EcR-B1 (B, D, and F) in the imaginal rings of the foregut (A and B), hindgut (C and D), and salivary gland (E and F). EcR-A is expressed at a higher level in the imaginal rings (arrows) of the foregut (A), hindgut (C), and salivary gland (E) than in the associated strictly larval tissues, including larval foregut and midgut (A), midgut and anterior hindgut (C), and salivary gland (E). EcR-B1 is expressed at lower levels in these imaginal rings than in the associated strictly larval tissues. Note, however, that the anti-B1 staining of the salivary gland ring is greater than that for the other two imaginal rings, making the anti-A to anti-B1 staining ratio for this imaginal tissue the lowest among these imaginal tissues, though still greater than 1. Although it is not visible in (D), the Malpighian tubules express EcR-B1 at a level comparable to that in the strictly larval tissues. 15G1a was used to immunolocalize EcR-A (A, C, and E), and AD4.4 was used for EcR-B1 localization (B, D, and F). All tissues were dissected from white prepupae.

EcR-B1 protein was observed in the second half of the second larval instar on longer exposure (data not shown).

A major peak of *EcR-A* mRNA expression was observed during the first day of pupal development, which was followed by a small peak during the last day (Figure 7A; 132–156 hr and 180–192 hr, respectively). By contrast, the pupal expression of the *EcR-B1* mRNA appears to be almost the reciprocal of the *EcR-A* mRNA expression, showing a modest peak at 156–168 hr. In spite of these differences in mRNA expression patterns, there appear to be little if any significant differences in the respective protein patterns during pupal development (Figure 7B, samples P-1 to P-7). This suggests that the turnover rates for these EcR proteins may be lower in pupae than at earlier times in development. More rapid turnover rates at the end of larval life, in prepupae, or both may, for example, account for the EcR-B1 degradation products observed in the L3-4 sample of Figure 7B.

Discussion

Structure and Function of *EcR* and Its Receptor Proteins

At first sight (Koelle et al., 1991), the *EcR* gene appeared to consist of a single transcription unit that encoded a single receptor protein. *EcR* was therefore thought to lack the structural and functional complexity of three of its target genes that had been cloned: the early genes *E74* (Burtis et al., 1990; Thummel et al., 1990), *E75* (Segraves and Hogness, 1990; Segraves, 1991), and *BR-C* (DiBello et al., 1991). Each of these genes encodes multiple structurally overlapping proteins from multiple overlapping transcrip-

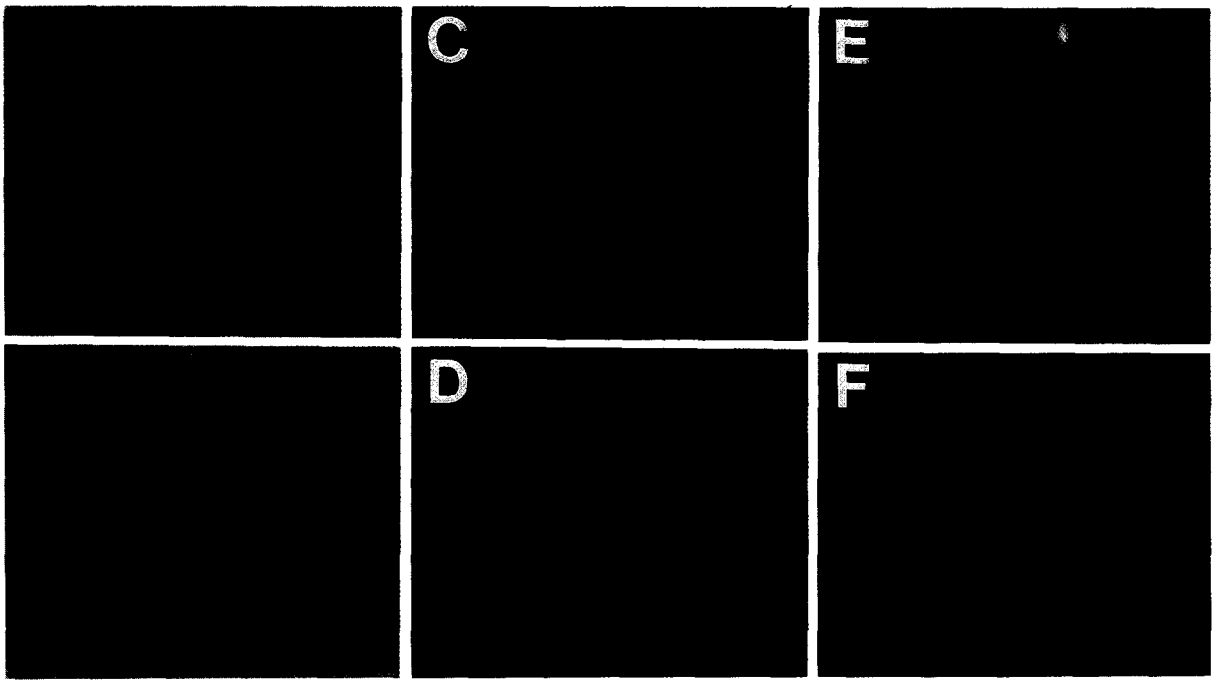

Figure 6. EcR-A and EcR-B1 Expression in the Cells of the Imaginal Midgut Islands and the Abdominal Histoblasts

Immunolocalization of EcR-A (A and C) and EcR-B1 (B and D) in the midgut (A and B) and epidermis (C and D). The islands of imaginal midgut cells express EcR-B1 (small cells in [B]) and do not express EcR-A at detectable levels. The larval midgut cells (large cells in [A] and [B]) are similar to most other strictly larval cell types, expressing high levels of EcR-B1 and low levels of EcR-A. Since our standard immunohistochemical-labeling conditions produce high background in cuticle preparations, EcR-A and EcR-B1 expression in the epidermis was examined by immunofluorescence. EcR-A and EcR-B1 antibody stains are shown in (C) and (D), respectively, and stains of the same fields of cells with the DNA-specific dye DAPI are shown in (E) and (F). The abdominal histoblasts are small cells that are weakly labeled by DAPI, owing to their diploid DNA content, whereas the polytene larval epidermal cells are relatively large and heavily labeled by DAPI. Both of these cell types express EcR-B1 (D), while neither expresses detectable levels of EcR-A. It is possible that either or both of these epidermal cell types express EcR-A at a level below the sensitivity of the immunofluorescence-labeling method, since this procedure is not as sensitive as the immunoperoxidase staining used for other cell types. Tissues in (A) and (B) were dissected from white prepupae, whereas those shown in (C) through (F) were dissected from wandering third instar larvae.

tion units and, in the case of the *BR-C* gene, from alternatively spliced products of these units. Consequently, the first focus of tissue diversity in the tissue coordination model was originally postulated to derive from different combinations of early gene proteins (Burtis et al., 1990).

In this paper we have shown that the *EcR* gene exhibits the same level of complexity as that of the early genes. Thus, we have found that the previously observed *EcR-B* transcript is alternatively spliced to yield the EcR-B2 isoform in addition to the previously observed EcR-B1 protein. We have also discovered the *EcR-A* transcription unit that overlaps the *EcR-B* unit encodes the EcR-A isoform and increases the length of the *EcR* gene 2-fold to ~73 kb (Figure 1), placing it in the same range as the early genes, which vary from ~60 kb for *E74* to ~100 kb for *E75* and *BR-C*. Consequently, the first focus of diversity among the ecdysone response hierarchies has been shifted to different combinations of the EcR protein isoforms.

The primary structure of each of the three EcR isoforms is divisible into two regions: a common 652 amino acid C-terminal region that includes the DNA-binding domain (66 amino acids) and the hormone-binding domain (221 amino acids) and an isoform-specific N-terminal domain of 197 (EcR-A), 226 (EcR-B1), or 17 (EcR-B2) amino acids (Figure 3A). Given these structures, the three EcR isoforms would, under the simplest assumptions, be expected to exhibit similar or identical DNA and hormone binding activities. In vitro binding studies using EcR isoforms synthesized in yeast demonstrate that this is indeed the case, providing that the EcR pairing partner, USP, is also present (Koelle, 1992; Koelle et al., 1993). We have shown that a minimal promoter carrying the ecdysone response element defined by Riddihough and Pelham (1987; this ecdysone response element was also used in the above DNA binding experiments) can be activated in an ecdysone-dependent manner by transfection of Drosophila cells deficient in EcR, but not in USP, with an expression construct for any of the three EcR isoforms (Table 2).

The above results indicate that the DNA and hormone binding activities of the EcR isoforms are relatively insensitive to differences in the isoform-specific N-terminal sequences. They also suggest that this is the case for the EcR activation of a simple synthetic promoter, although it should be noted that the data in Table 2 do not allow quantitative comparison of the activities of the EcR iso-

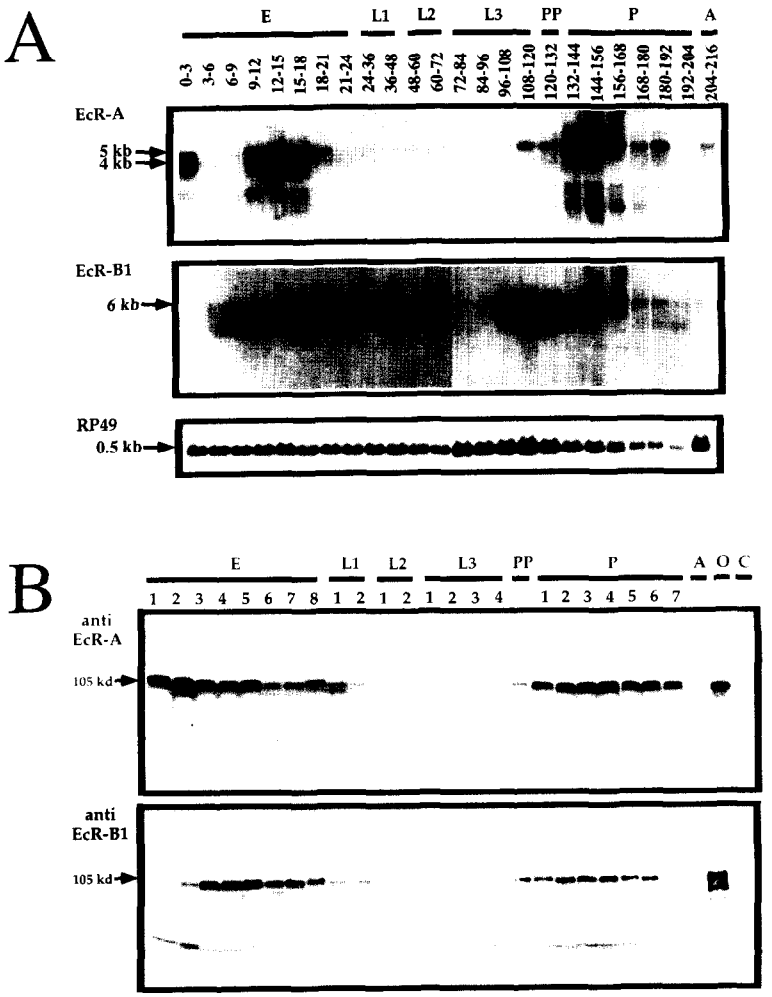

Figure 7. Temporal Expression Patterns of the *EcR-A* and *EcR-B1* mRNAs and Proteins

(A) Northern analysis. A Northern filter with total RNA from animals at the indicated stages was serially hybridized with *EcR-A* (top panel) and *EcR-B1* (middle panel) DNA probes. An *RP49* probe (O'Connell and Rosbash, 1984) was used to control for RNA loading differences (bottom panel). The hours and stages of development are shown at the top of the figure: E, embryos; L1, L2, and L3, the three larval instars; PP, prepupae; P, pupae; A, adults.

(B) Western analysis. Similarly prepared Western filters with protein from animals at the indicated stages of development were probed with the EcR-A-specific antibody 15G1a (top panel) or the EcR-B1 specific antibody AD4.4 (bottom panel). The protein samples are labeled differently from the RNA samples in (A) to emphasize that they derived from different sets of animals, although they were collected at the same time intervals: every 3 hr during embryogenesis and approximately every 12 hr thereafter. To show that the proteins recognized by these antibodies comigrate with the appropriate EcR proteins produced in cultured cells, extracts from EcR overexpressor (lanes O) and control (lanes C) cultured cells were coelectrophoresed with the Drosophila extracts (see Experimental Procedures). In addition to the 105 kd EcR-B1 protein, AD4.4 detects a protein of lower apparent molecular size (~65 kd) that is present in S2 cells (data not shown) and in animals of many stages. Since this protein is not recognized by common region antibodies (data not shown), it does not correspond to any characterized *EcR* gene product, and it may therefore be a fortuitously cross-reactive antigen. Presumptive EcR-B1 breakdown products have been detected in independently prepared extracts of wandering third instar larvae (lanes L3-4). One of these extracts was examined and found to contain full-length E74A protein (S. Munroe and D. S. H., unpublished data), suggesting that these EcR-B1 breakdown products result from protein turnover in vivo and not from faulty extract preparation. On both the EcR-A and EcR-B1 filters, total protein was underloaded ~2-fold in lanes L2-1, L2-2, L3-1, L3-2, L3-3, and A.

forms since the abundance of each isoform in the transfected cells was not determined. In any case, the data raise the question as to whether the EcR isoforms can differentially regulate more complex promoters in different cell types.

There is precedent for such a distinction between the effects of N-terminal regions on the activation of simple synthetic promoters in a given cell type and on complex promoters in multiple cell types. Two vertebrate members of the steroid receptor superfamily, the estrogen and progesterone receptors, have been shown to contain promoter- and cell type–specific transcriptional activation domains in their N-terminal regions (Tora et al., 1988, 1989; Kastner et al., 1990). Specifically, Kastner et al. (1990) found that the transcription of the progestin responsive ovalbumin gene promoter can be induced by the A isoform of the human progesterone receptor, but not by the B isoform. Conversely, the human progesterone receptor B isoform activates the mouse mammary tumor virus long terminal repeat promoter more efficiently than does human progesterone receptor A. Furthermore, the two human progesterone receptor isoforms do not differ significantly in their abilities to activate a synthetic reporter construct containing a single palindromic progestin response element (Kastner et al., 1990). We make use of this precedent in the next section, where we analyze the tissue distributions of the EcR-A and EcR-B1 isoforms.

Are Different Combinations of the EcR Isoforms Required for Different Tissue Responses to Ecdysone?

While virtually all tissues exhibit some kind of morphological change in response to the metamorphic ecdysone pulse that peaks at the end of larval life (Bodenstein, 1950), only a fraction of these tissues have been examined in organ culture to determine whether that response is direct. Cultured imaginal discs have been shown to differentiate in response to ecdysone (Fristrom et al., 1973), and cultured larval salivary glands and fat bodies are induced by ecdysone to initiate temporal patterns of chromosome

puffing that mimic those observed in vivo (Ashburner et al., 1974; Richards, 1982). In most cases, however, such demonstrations of a direct ecdysone response either have not yet been carried out or are extremely difficult to carry out because of cell-to-cell contacts between tissue types, as, for example, in the case of the imaginal midgut islands and the larval midgut (Figures 6A and 6B). In the following analysis, we have not distinguished between tissues that have or have not been demonstrated to respond directly to ecdysone. However, since we are concerned only with tissues that express ecdysone receptors, we are, in effect, assuming that tissues that express an ecdysone receptor isoform respond directly to ecdysone. In this regard, it should be noted that USP is expressed in all of these tissues and, indeed, appears to be ubiquitous at this stage of development (W. S. T., unpublished data).

The most striking characteristic of the EcR-A and EcR-B1 expression patterns at the onset of metamorphosis (i.e., in white prepupae) is that tissues belonging to the same metamorphic class exhibit the same expression pattern. For example, the imaginal discs form an obvious metamorphic class, and the different discs uniformly exhibit a high anti-A to anti-B1 staining ratio (Figures 4A and 4B). Similarly, the imaginal cells of the midgut islands and histoblast nests also form a clear metamorphic class characterized by massive cell multiplication and migration that is quite distinct from the disc response (Bodenstein, 1950; Madhavan and Schneiderman, 1977; Roseland and Schneiderman, 1979). Their antibody staining pattern exhibits the highest anti-B1 to anti-A ratio that we have observed; indeed, significant anti-A staining was not detected (Figure 6). The strictly larval tissues can also be viewed as a metamorphic class, although of more general definition than the above imaginal classes. With the notable exception of the prothoracic gland, they exhibit a high anti-B1 to anti-A staining ratio (Figures 4–6).

We propose that the above correlations result from the requirement of particular EcR isoforms, or combinations thereof, for particular metamorphic responses. We suppose that these receptor isoforms complex with ecdysone to activate genetic regulatory hierarchies required for a particular metamorphic response, hierarchies that include particular combinations of activated early genes that express combinations of transcription factors that in turn specify the larger combinations of late gene proteins required to effect the response.

Recent mutational analyses of *EcR* support the proposal that particular metamorphic responses require particular EcR isoforms. According to this proposal, isoform-specific mutations would be expected to uncouple metamorphosis, allowing tissues that do not express the particular isoform to initiate metamorphosis, while preventing the metamorphosis of tissues that express the isoform, given that it is required for their metamorphosis. Such an uncoupling has been observed in EcR-B1-specific mutants (M. Bender, W. S. T., and D. S. H., unpublished data). More specifically, the imaginal discs, where EcR-A predominates, initiate metamorphosis normally in these EcR-B1 mutants, while the larval tissues, in which EcR-B1 normally predominates, do not. This uncoupling of metamorphosis in EcR-B1 mutants can be reversed by expression of EcR-B1 from transgenic constructs, but not by the similar expression of the other two isoforms.

Further support for the proposal derives from an interesting correlation between isoform expression and an ecdysone-regulated fate at the single cell level (S. Robinow, W. S. T., D. S. H., and J. W. Truman, unpublished data). These cells consist of a heterogeneous group of ~300 neurons in the central nervous system that uniquely express a 10-fold higher level of EcR-A than do other central neurons during the pupal stage of development. These neurons were observed to share the same unique fate of rapid degeneration after adult emergence from the pupal case, a fate that requires the decrease in ecdysone titer that occurs at the end of pupal development.

While tissues belonging to the same metamorphic class exhibit the same EcR-A and EcR-B1 expression patterns, the reciprocal statement is not valid. Thus, EcR-B1 predominates over EcR-A both in larval tissues and in imaginal histoblast nests and midgut islands, tissues that belong to quite different metamorphic classes. Similarly, EcR-A predominates over EcR-B1 in imaginal discs, the larval prothoracic gland, and the above neurons, again tissues with quite different metamorphic responses to ecdysone. This lack of reciprocity suggests that factors other than EcR-A and EcR-B1 are required to specify the metamorphic response to ecdysone. Clearly, the EcR-B2 isoform is a likely candidate for such a factor, a likelihood that we cannot address at the moment because EcR-B2-specific antibodies are not available.

Other possible factors that could account for this lack of reciprocity are those that might alter the function of the EcR proteins. For example, if the USP protein were limiting in certain cells, it could change the distribution of EcR functions were the EcR isoforms to exhibit different binding coefficients for USP. Alternatively, other Drosophila members of the steroid receptor superfamily, many of which have been identified (Segraves, 1991), might be able to substitute for USP as pairing partners for the EcR proteins and thereby change the EcR functions. Support for this possibility comes from an analysis of mitotic clones that suggests that wild-type *usp* function is not required for the development of the adult cuticular structures of the notum and abdomen (Oro et al., 1992). By contrast, examination of transheterozygotes for usp^- and EcR^- null mutations shows that they exhibit defective wing phenotypes, suggesting that both *usp* and *EcR* functions are required for normal metamorphosis of the wing imaginal disc, which also yields the notum (M. Bender and D. S. H., unpublished data).

Recent work on a vertebrate steroid receptor, the glucocorticoid receptor, suggests that transcription factors that are not members of the steroid receptor superfamily might also complex with the EcR proteins and modify their activities. Both octomer transcription factor 1, a homeodomain protein, and AP-1, a heterodimer of the Fos and Jun leucine zipper proteins, can complex with the glucocorticoid receptor and inhibit its DNA binding activity (Jonat et al., 1990; Yang-Yen et al., 1990; Kutoh et al., 1992). AP-1 has been proposed similarly to antagonize the activities of the

retinoic acid, thyroid hormone, and estrogen receptors (Desbois et al., 1991; Doucas et al., 1991; Schüle et al., 1991; Zhang et al., 1991), suggesting that Drosophila homeodomain and leucine zipper proteins could complex with the EcR proteins and alter their activites.

This consideration of the possible mechanisms for altering the functions of a given combination of EcR isoforms, as well as the observation that tissues belonging to an obvious metamorphic class (e.g., imaginal discs) express the same combination, raises the question of how many different ecdysone-responsive genetic regulatory hierarchies are employed to effect metamorphosis. We are not concerned here with the short, truncated "hierarchies" consisting of *EcR* and a primary ecdysone responsive gene that cannot extend the hierarchy because it does not encode a genetic regulatory protein, i.e., genes like *Eip28/29*, *IMP-E2*, and *Fbp-1* (Cherbas et al., 1986; Paine-Saunders et al., 1990; Deutsch et al., 1989). While such genes may make a significant contribution to the tissue response, their number appears to be quite small in comparison to the late genes, which, as registered by the late puffs, are in the hundreds for a single tissue.

The question can be framed in more specific terms if we limit it to the set of imaginal discs. Thus, we can ask, is the metamorphosis of each of the ten kinds of discs directed by a different ecdysone responsive hierarchy, or do all ten employ the same hierarchy? In the latter case, the morphological differences in the responses of different discs might derive from a common set of late gene proteins from the hierarchy acting in the context of different intracellular and extracellular structures built into each disc according to directions provided by earlier acting genes, such as the homeotic genes. Thus, the change in the metamorphic response of the antenna disc to that normally reserved for a leg disc by the expression of either the *Antennapedia* (Gibson et al., 1990) or *Ultrabithorax* (Mann and Hogness, 1990) homeotic genes at the time of the second to third instar larval molt might result solely from such structural changes without change of the ecdysone response hierarchy. Alternatively, the expression of these homeotic genes may cause the synthesis of factors, such as those noted above, that would change the function of the EcR proteins, thereby changing the hierarchy from that used to direct antenna disc metamorphosis to that used for leg disc metamorphosis. These are testable alternatives that we look forward to resolving.

Experimental Procedures

Isolation and Analysis of cDNA and Genomic Clones

Recombinant DNA procedures were performed by standard methods (Sambrook et al., 1989). DNA sequencing was performed as described by Koelle et al. (1991).

EcR-A and *EcR-B2* cDNA clones were isolated from a λgt10 cDNA library constructed from third instar larval tissues that had been cultured with ecdysone and cycloheximide (a gift from C. Thummel) as plaques that hybridized to a common region probe (base pairs 1752–2251 of the *EcR-B1* cDNA sequence [Koelle et al., 1991]) and that failed to hybridize to an *EcR-B1*-specific probe (base pairs 1270–1731). The *EcR-A*-specific region of one cDNA clone (pWT57) was sequenced on both strands. The exon 1 to exon 3 junction of an *EcR-B2* clone (pWT56) was sequenced to confirm that this splice is made from the same donor and acceptor sequences used in *EcR-B1*.

Genomic clones containing the *EcR-A*-specific exons were obtained using *EcR-A* cDNA fragments and previously isolated *EcR* genomic clones as probes to screen genomic phage libraries. Genomic phages 2.1, 2.2, 6.1, and 2.10 were isolated from the library of Maniatis et al. (1978); 3.9.1 was isolated from the library of Moses et al. (1989). Exon-bearing fragments were identified by hybridization to *EcR-A* cDNA probes. The genomic sequence of each of the three *EcR-A*-specific exons was entirely determined on one strand and compared with the *EcR-A* cDNA sequence to identify the exon boundaries.

Primer Extension and Ribonuclease Protection Analyses

Primer extension assays were performed with ^{32}P-end-labeled oligonucleotide primers either by the method of Sambrook et al. (1989) or by that of Johnson and Krasnow (1990). The *EcR-A* primer (5′-TCGATTGGCCTCAAAATGTTTCTTAGACCC-3′) was complementary to nucleotides 105–134 of the sequence presented in Figure 2A. The *EcR-B* primer (5′-GCTTTGGGAAACCGTACTGTTAGGTTGTCG-3′) was complementary to nucleotides 108–137 of the sequence shown in Figure 2B. The same primers were used on cloned genomic DNA templates to generate dideoxy sequencing ladders that were compared with the primer extension products to determine the *EcR-A* and *EcR-B* transcription initiation sites.

The transcription initiation site assignments based on the primer extension analyses were confirmed by ribonuclease protection experiments with antisense genomic RNA probes that spanned the 5′ ends of the *EcR-A* and *EcR-B* transcription units (Talbot, 1993). The *EcR-A* probe was complementary to nucleotides −129 to +202 of the sequence in Figure 2A, and the *EcR-B* probe was complementary to nucleotides −92 to +190 of the sequence shown in Figure 2B. Ribonuclease protection experiments were performed with the RPA II kit (Ambion) according to the instructions of the manufacturer.

Plasmid Construction

The EcR-A and EcR-B2 expression constructs were derived from the actin 5C promoter expression plasmid pAct/SV40/BS (Koelle et al., 1991). To generate pAct/EcR-B2, the BamHI–EcoRI fragment of the *EcR-B2* cDNA clone pWT56, which contains the entire *EcR-B2* open reading frame (ORF), was inserted into the EcoRV site of pAct/SV40/BS, after filling the incompatible ends with Klenow fragment. Two similar EcR-A expression constructs, pAct/EcR-A/1 and pAct/EcR-A/2, were constructed from two different *EcR-A* cDNAs. pAct/EcR-A/1 was constructed by inserting the NdeI–EcoRI fragment of the *EcR-A* cDNA pWT57, which contains the entire *EcR-A* ORF, into the EcoRV site of pAct/SV40/BS, after filling the incompatible ends with Klenow fragment. pAct/EcR-A/2 was constructed by inserting the NdeI–HindIII fragment of the *EcR-A* cDNA clone pWT100, which contains the entire *EcR-A* ORF, into the EcoRV site of pAct/SV40/BS, after filling the incompatible ends with Klenow fragment. Both of these clones express the EcR-A polypeptide identified in Figure 3B, and they have been used interchangably. pAct/EcR-A/1 was used in the experiment presented in Table 2; pAct/EcR-A/2 was used for the experiments shown in Figures 3B and 7B.

pEAS3 is an Escherichia coli expression plasmid that produces a TrpE–EcR-B1 fusion protein containing both isoform-specific and common segments of EcR-B1 (residues 68–878). To construct pEAS3, the appropriate StyI–HindIII fragment of the *EcR-B1* cDNA pMK1 was inserted into pATH2 (Rimm and Pollard, 1989) that had been cleaved with SmaI and HindIII, after blunting the StyI end.

pWT73 is an E. coli expression plasmid that produces a β-galactosidase (β-gal)–EcR-A fusion protein containing residues 15–199 of EcR-A, of which all but residues 198 and 199 are form specific. To construct pWT73, the appropriate SalI–NruI *EcR-A* cDNA fragment was inserted into pUR278 (Ruther and Muller, 1983) that had been cleaved with SalI and HindIII, after blunting the HindIII end.

Additional TrpE–EcR and β-gal–EcR fusion protein expression plasmids were constructed for use in the monoclonal antibody epitope localization experiments. The names of the TrpE–EcR-B1 fusion protein expression plasmids and the EcR-B1 residues that they encode follow: pWT48, amino acids 68–649; pWT49, amino acids 68–393; pWT46, amino acids 68–222; pWT47, amino acids 649–878; pWT44, amino acids 222–878; pMK24, amino acids 335–447; and pWT102, amino acids 222–331. These clones were constructed either by deleting the appropriate *EcR-B1* coding sequences from pEAS3 or by in-

serting the appropriate *EcR-B1* cDNA fragments into pATH–TrpE fusion vectors (Rimm and Pollard, 1989). The β-gal–EcR-A fusion protein expression plasmid pWT74A encodes residues 15–152 of the EcR-A protein and was constructed by inserting the appropriate SalI–BstNI *EcR-A* cDNA fragment into pUR278 (Ruther and Muller, 1983) that had been cleaved with SalI and HindIII, after blunting the BstNI and HindIII ends.

Transfection and Hormonal Induction of Cultured Cells

Ecdysone-resistant S2 cells were cultured and transfected as described by Koelle et al. (1991). The actin 5C expression vectors described above and the pAct–EcR-B1 construct reported by Koelle et al. (1991) were used to express the EcR proteins in transiently transfected cultured cells. The pEcRE/Adh/βgal reporter plasmid (Koelle et al., 1991) was cotransfected with each EcR expression construct. Each transfected culture was split into two dishes, one of which was treated with 20-OH ecdysone while the other was not. E. coli β-gal activity produced from the pEcRE/Adh/βgal reporter plasmid was assayed as described by Koelle et al. (1991), and the activities of the treated and untreated samples from each dish of transfected cells were compared to obtain the fold ecdysone induction.

Preparation of Anti-EcR Antibodies and Epitope Localization

The TrpE–EcR-B1 fusion protein expressed by pEAS3 was used as the immunogen to produce the EcR-B1-specific and common region monoclonal antibodies listed in Table 1. The EcR-A-specific monoclonal antibodies (Table 1) were raised against the pWT73 β-gal–EcR-A fusion protein. Fusion proteins were prepared for immunization as described (Koelle et al., 1991).

For the production of monoclonal antibodies, mice were immunized and hybridomas were generated as described by Lopez and Hogness (1991). Hybridoma supernatants were screened by enzyme-linked immunosorbent assay for reactivity to EcR fusion proteins, and clones that were positive initially were rescreened by immunoblotting. Hybridoma lines producing anti-EcR monoclonal antibodies were cloned by limiting dilution.

All of the common region antibodies listed in Table 1 were tested by immunoblot experiments similar those shown in Figure 3B, and each was found to recognize all three of the EcR isoforms (data not shown). The specificity of the EcR-A antibodies was demonstrated in similar experiments in which the antibodies were tested for reactivity against EcR-A and at least one of the EcR-B forms and found to recognize only EcR-A (Figure 3B; data not shown). The locations of the anti-EcR monoclonal antibody epitopes were determined by testing for immunoblot reactivity to E. coli fusion proteins containing various segments of the EcR isoform–specific and common regions (expression constructs described above). The results of this analysis are summarized in Table 1.

Northern Analysis

The developmental Northern filter prepared by Thummel et al. (1990) was serially rehybridized with ^{32}P-labeled double-stranded DNA probes, allowing time for the signal to decay between experiments. The *EcR-A* probe was a cDNA fragment containing base pairs 17–982 of the nucleotide sequence presented in Figure 2; this fragment is composed of *EcR-A* specific sequences, with the exception of the last four nucleotides, which derive from the common region of the cDNA. The *EcR-B1*-specific probe contained base pairs 1270–1731 of the *EcR-B1* cDNA sequence (Koelle et al., 1991). The *RP49* loading control has been reported previously (Koelle et al., 1991) and is shown again here to aid comparison.

Western Analysis

Samples were prepared and immunoblots were done as described previously (Koelle et al., 1991). The extracts used for EcR-A and EcR-B1 overexpressor and control lanes in the developmental Western blots shown in Figure 7B are given below. The EcR-A overexpressor extract (Figure 7B, lane O, anti-EcR-A) was prepared from S2 cells transiently transfected with pAct/EcR-A/2, and the control (Figure 7B, lane C, anti-EcR-A) was prepared from S2 cells transfected with pAct/EcR-B1. The EcR-B1 overexpressor and control extracts were prepared from S2 cells stably transfected with EcR-B1 and DHR3 (another Drosophila steroid receptor homolog [Koelle et al., 1992]) expression constructs, respectively; the endogenous EcR-B1 that is present in these cells is not detected under the conditions used for these immunoblots. Total protein in lanes O and C of the EcR-B1 filter were both underloaded ~10-fold so that the signal intensity of the stably transfected EcR-B1-expressing cell line would be comparable to the other samples.

Immunolocalization

For antibody stains of larvae and prepupae, animals were dissected in phosphate-buffered saline and fixed in 2% formaldehyde. The subsequent steps were performed essentially as described (Ashburner, 1989), with the modifications noted below. Tissues were incubated with primary and secondary antibodies for 12–18 hr at room temperature. Anti-EcR hybridoma culture supernatants were diluted 1:10. Peroxidase-coupled secondary antibodies (Bio-Rad) were diluted 1:2000. For the immunofluorescence experiments shown in Figure 6, rhodamine-conjugated secondary antibodies (Jackson Laboratory) were diluted 1:200; after immunostaining, these tissues were briefly treated with the DNA-specific dye DAPI (1 μg/ml) as a counterstain. Immunostaining results similar to those shown in Figures 4–6 were obtained reproducibly in independent trials.

Acknowledgments

We are grateful to Jim Truman for many helpful discussions and for communication of his unpublished data. We thank Ken Burtis for the developmental Northern blot, John Chuang for embryonic RNA samples, Carl Thummel for the cDNA library, and Mark Krasnow, Daria Siekhaus, Michael Bender, Michael Koelle, and Monica Gorman for helpful discussions and comments on the manuscript. W. S. T. was supported by a National Science Foundation graduate fellowship and a National Insitutes of Health (NIH) training grant. This work was supported by a grant from the NIH to D. S. H.

Received March 16, 1993; revised April 23, 1993.

References

Ashburner, M. (1989). *Drosophila*: A Laboratory Manual (Cold Spring Harbor, New York: Cold Spring Harbor Laboratory Press).

Ashburner, M., Chihara, C., Meltzer, P., and Richards, G. (1974). Temporal control of puffing activity in polytene chromosomes. Cold Spring Harbor Symp. Quant. Biol. *38*, 655–662.

Bate, M., and Martinez-Arias, A. (1991). The embryonic origin of imaginal discs in *Drosophila*. Development *112*, 755–761.

Bodenstein, D. (1950). The post-embryonic development of *Drosophila*. In Biology of *Drosophila*, M. Demerec, ed. (New York: Hafner), pp. 275–367.

Burtis, K. C. (1985). Isolation and characterization of an ecdysone inducible gene from *Drosophila melanogaster*. Ph. D. thesis, Stanford University, Stanford, California.

Burtis, K. C., Thummel, C. S., Jones, C. W., Karim, F. D., and Hogness, D. S. (1990). The Drosophila 74EF early puff contains *E74*, a complex ecdysone-inducible gene that encodes two *ets*-related proteins. Cell *61*, 85–99.

Cherbas, L., Schulz, R. A., Koehler, M. M., Savakis, C., and Cherbas, P. (1986). Structure of the *Eip28/29* gene, an ecdysone-inducible gene from *Drosophila*. J. Mol. Biol. *189*, 617–631.

Christopherson, K. S., Mark, M. R., Bajaj, V., and Godowski, P. J. (1992). Ecdysteroid-dependent regulation of genes in mammalian cells by a *Drosophila* ecdysone receptor and chimeric transactivators. Proc. Natl. Acad. Sci. USA *89*, 6314–6318.

Condic, M. L., Fristrom, D., and Fristrom, J. W. (1991). Apical cell shape changes during *Drosophila* imaginal leg disc elongation: a novel morphogenetic mechanism. Development *111*, 23–33.

Desbois, C., Aubert, D., Legrand, C., Pain, B., and Samarut, J. (1991). A novel mechanism of action for v-ErbA: abrogation of the inactivation of transcription factor AP-1 by retinoic acid and thyroid hormone receptors. Cell *67*, 731–740.

Deutsch, J., Laval, M., Lepesant, J. A., Maschat, F., Pourrain, F., and

Rat, L. (1989). Larval fat body-specific gene expression in *D. melanogaster*. Dev. Genet. *10*, 221–231.

DiBello, P. R., Withers, D. A., Bayer, C. A., Fristrom, J. W., and Guild, G. M. (1991). The *Drosophila Broad-Complex* encodes a family of related proteins containing zinc fingers. Genetics *129*, 385–397.

Doucas, V., Spyrou, G., and Yaniv, M. (1991). Unregulated expression of c-Jun or c-Fos proteins but not Jun D inhibits estrogen receptor activity in human breast cancer derived cells. EMBO J. *10*, 2237–2245.

Fristrom, J. W., Logan, W. R., and Murphy, C. (1973). The synthetic and minimal culture requirements for evagination of imaginal discs of *Drosophila melanogaster in vitro*. Dev. Biol. *33*, 441–456.

Fristrom, J. W., Fristrom, D., Fekete, E., and Kuniyuki, A. H. (1977). The mechanism of evagination of imaginal discs of *Drosophila melanogaster*. Am. J. Zool. *17*, 671–684.

Gibson, G., Schier, A., LeMotte, P., and Gehring, W. J. (1990). The specificities of Sex combs reduced and Antennapedia are defined by a distinct portion of each protein that includes the homeodomain. Cell *62*, 1087–1103.

Guay, P. S., and Guild, G. M. (1991). The ecdysone-induced puffing cascade in *Drosophila* salivary glands: a *Broad-Complex* early gene regulates intermolt and late gene transcription. Genetics *129*, 169–175.

Johnson, F. B., and Krasnow, M. A. (1990). Stimulation of transcription by an Ultrabithorax protein *in vitro*. Genes Dev. *4*, 1044–1052.

Jonat, C., Rahmsdorf, H. J., Park, K.-K., Cato, A. C. B., Gebel, S., Ponta, H., and Herrlich, P. (1990). Antitumor promotion and antiinflammation: down-modulation of AP-1 (Fos/Jun) activity by glucocorticoid hormone. Cell *62*, 1189–1204.

Karim, F. D., and Thummel, C. S. (1991). Ecdysone coordinates the timing and amounts of *E74A* and *E74B* transcription in *Drosophila*. Genes Dev. *5*, 1067–1079.

Karim, F. D., and Thummel, C. S. (1992). Temporal coordination of regulatory gene expression by the steroid hormone ecdysone. EMBO J. *11*, 4083–4093.

Kastner, P., Krust, A., Turcotte, B., Stropp, U., Tora, L., Gronemeyer, H., and Chambon, P. (1990). Two distinct estrogen-regulated promoters generate transcripts encoding the two functionally different human progesterone receptor forms A and B. EMBO J. *9*, 1603–1614.

Koelle, M. R. (1992). Molecular analysis of the *Drosophila* ecdysone receptor complex. Ph. D. thesis, Stanford University, Stanford, California.

Koelle, M. R., Talbot, W. S., Segraves, W. A., Bender, M. T., Cherbas, P., and Hogness, D. S. (1991). The Drosophila *EcR* gene encodes an ecdysone receptor, a new member of the steroid receptor superfamily. Cell *67*, 59–77.

Koelle, M. R., Segraves, W. A., and Hogness, D. S. (1992). DHR3: A *Drosophila* steroid receptor homolog. Proc. Natl. Acad. Sci. USA *89*, 6167–6171.

Koelle, M. R., Arbeitman, M., and Hogness, D. S. (1993). Hormone and DNA binding by *Drosophila* ecdysone receptors requires EcR/Ultraspiracle complexes. Proc. Natl. Acad. Sci. USA *90*, in press.

Kutoh, E., Strömstedt, P.-E., and Poellinger, L. (1992). Functional interference between the ubiquitous and constitutive octamer transcription factor 1 (OTF-1) and the glucocorticoid receptor by direct protein–protein interaction involving the homeo subdomain of OTF-1. Mol. Cell. Biol. *12*, 4960–4969.

Lopez, A. J., and Hogness, D. S. (1991). Immunochemical dissection of the Ultrabithorax homeoprotein family in *Drosophila melanogaster*. Proc. Natl. Acad. Sci. USA *88*, 9924–9928.

Madhavan, M. M., and Schneiderman, H. A. (1977). Histological analysis of the dynamics of growth of imaginal discs and histoblast nests during the larval development of *Drosophila melanogaster*. Roux's Arch. Dev. Biol. *183*, 269–305.

Maniatis, T., Hardison, R. C., Lacy, E., Lauer, J., O'Connell, C., Quon, D., Sim, G. K., and Efstratiadis, A. (1978). The isolation of structural genes from libraries of eucaryotic DNA. Cell *15*, 687–701.

Mann, R. S., and Hogness, D. S. (1990). Functional dissection of the Ultrabithorax proteins in D. melanogaster. Cell *60*, 597–610.

Moses, K., Ellis, M. C., and Rubin, G. M. (1989). The *glass* gene encodes a zinc-finger protein required by *Drosophila* photoreceptor cells. Nature *340*, 531–536.

Mount, S. M. (1982). A catalogue of splice junction sequences. Nucl. Acids Res. *10*, 459–472.

O'Connell, P. O., and Rosbash, M. (1984). Sequence, structure, and codon preference of the *Drosophila* ribosomal protein 49 gene. Nucl. Acids Res. *12*, 5495–5513.

Oro, A. E., McKeown, M., and Evans, R. M. (1992). The *Drosophila* retinoid X receptor homolog *ultraspiracle* functions in both female reproduction and eye morphogenesis. Development *115*, 449–462.

Paine-Saunders, S., Fristrom, D. K., and Fristrom, J. W. (1990). The *Drosophila IMP-E2* gene encodes an apically secreted protein expressed during imaginal disc morphogenesis. Dev. Biol. *140*, 337–351.

Richards, G. P. (1981). The radioimmune assay of ecdysteroid titres in *Drosophila melanogaster*. Mol. Cell. Endocrinol. *21*, 181–197.

Richards, G. P. (1982). Sequential gene activation by ecdysteroids in polytene chromosomes of *Drosophila melanogaster*. VII. Tissue specific puffing. Roux's Arch. Dev. Biol. *191*, 103–111.

Riddiford, L. M. (1993). Hormones and *Drosophila* development. In The Development of *Drosophila*, M. Bate and A. Martinez-Arias, eds. (Cold Spring Harbor, New York: Cold Spring Harbor Laboratory Press), in press.

Riddihough, G., and Pelham, H. R. B. (1987). An ecdysone response element in the *Drosophila hsp27* promoter. EMBO J. *6*, 3729–3734.

Rimm, D. L., and Pollard, T. D. (1989). New plasmid vectors for high level synthesis of eukaryotic fusion proteins in *Escherichia coli*. Gene *75*, 323–327.

Roseland, C. R., and Schneiderman, H. A. (1979). Regulation and metamorphosis of the abdominal histoblasts of *Drosophila melanogaster*. Roux's Arch. Dev. Biol. *186*, 235–265.

Ruther, U., and Muller, H. B. (1983). Easy identification of cDNA clones. EMBO J. *2*, 1791–1794.

Sakurai, S., and Gilbert, L. I. (1990). Biosynthesis and secretion of ecdysteroids by the prothoracic glands. In Molting and Metamorphosis, E. Ohnishi and H. Ishizaki, eds. (Tokyo: Japan Science Society Press), pp. 83–106.

Sakurai, S., and Williams, C. M. (1989). Short-loop negative and positive feedback on ecdysone secretion by prothoracic gland in the tobacco hornworm, *Manduca sexta*. Gen. Comp. Endocrinol. *75*, 204–216.

Sambrook, J., Fritsch, E. F., and Maniatis, T. (1989). Molecular Cloning: A Laboratory Manual, Second Edition (Cold Spring Harbor, New York: Cold Spring Harbor Laboratory Press).

Schüle, R., Rangarajan, P., Yang, N., Kliewer, S., Ransone, L. J., Bolado, J., Verma, I. M., and Evans, R. M. (1991). Retinoic acid is a negative regulator of AP-1 responsive genes. Proc. Natl. Acad. Sci. USA *88*, 6092–6096.

Segraves, W. A. (1988). Molecular and genetic analysis of the *E75* ecdysone-responsive gene of *Drosophila melanogaster*. Ph. D. thesis, Stanford University, Stanford, California.

Segraves, W. A. (1991). Something old, some things new: the steroid receptor superfamily in Drosophila. Cell *67*, 225–228.

Segraves, W. A., and Hogness, D. S. (1990). The *E75* ecdysone-inducible gene responsible for the 75B early puff in *Drosophila* encodes two new members of the steroid receptor superfamily. Genes Dev. *4*, 204–219.

Talbot, W. S. (1993). Structure, expression, and function of ecdysone receptor isoforms in *Drosophila*. Ph. D. thesis, Stanford University, Stanford, California.

Thomas, H. E., Stunnenberg, H. G., and Stewart, A. F. (1993). Heterodimerisation of the *Drosophila* ecdysone receptor with retinoid X receptor and ultraspiracle. Nature *362*, 471–475.

Thummel, C. S., Burtis, K. C., and Hogness, D. S. (1990). Spatial and temporal patterns of *E74* transcription during Drosophila development. Cell *61*, 101–111.

Tora, L., Gronemeyer, Turcotte, B., Gaub, M.-P., and Chambon, P. (1988). The N-terminal region of the chicken progesterone receptor specifies target gene activation. Nature *333*, 185–188.

Tora, L., White, J., Brou, C., Tasset, D., Webster, N., Scheer, E., and Chambon, P. (1989). The human estrogen receptor has two independent nonacidic transcriptional activation functions. Cell *59*, 477–487.

Urness, L. D., and Thummel, C. S. (1990). Molecular interactions within the ecdysone regulatory hierarchy: DNA binding properties of the Drosophila ecdysone-inducible *E74A* protein. Cell *63*, 47–61.

Yang-Yen, H.-F., Chambard, J.-C., Sun, Y.-L., Smeal, T., Schmidt, T. J., Drouin, J., and Karin, M. (1990). Transcriptional interference between c-Jun and the glucocorticoid receptor: mutual inhibition of DNA binding due to direct protein–protein interaction. Cell *62*, 1205–1215.

Yao, T.-P., Segraves, W. A., Oro, A. E., McKeown, M., and Evans, R. M. (1992). Drosophila ultraspiracle modulates ecdysone receptor function via heterodimer formation. Cell *71*, 63–72.

Zhang, X.-K., Wills, K. N., Husmann, M., Hermann, T., and Pfahl, M. (1991). Novel pathways for thyroid hormone receptor action through interaction with *jun* and *fos* oncogene activites. Mol. Cell. Biol. *11*, 6016–6025.